

The characteristic stellar mass as a function of redshift

Cathie J. Clarke¹ and Volker Bromm^{1,2}

¹*Institute of Astronomy, Madingley Road, Cambridge CB3 0HA*

²*Harvard-Smithsonian Center for Astrophysics, 60 Garden Street, Cambridge, MA 02138, U.S.A.*

7 September 2018

ABSTRACT

We present a model for the star formation process during the initial collapse of dark matter haloes at redshifts $z = 0 - 30$. We derive a simple formula for the characteristic stellar mass scale during this initial burst of star formation. In our picture, this characteristic scale reflects both the minimum temperature to which the gas can cool (determined by the metallicity and the temperature of the cosmic microwave background) and the pressure of overlying baryons in the collapsing halo. This prescription reproduces both the large mass scales found in simulations of Population III star formation and the near solar values observed for star formation at low redshift.

Key words: cosmology: theory – early universe – galaxies: formation – stars: formation.

1 INTRODUCTION

It has long been recognised that the observed form of the initial mass function (IMF) in the Milky Way imprints the stellar population with a characteristic mass somewhat below $1M_{\odot}$. The existence of a characteristic scale, linked to neither the upper nor lower limits of the observed IMF, owes itself to the observed flattening of the mass function in this region (Scalo 1986, 1998; Kroupa, Tout & Gilmore 1990). If the IMF is parameterised by a series of disjoint power laws with respective indices α (such that the number of stars in the mass range m to $m + dm$ is $\propto m^{-\alpha} dm$), then the total mass contributed by each power law section is dominated by the upper (lower) mass limits of the section if α is respectively $< (>)$ 2. Since α makes the transition from ~ 2.35 to ~ 1.5 at around a solar mass, it follows that the characteristic stellar mass is around this value.

At higher masses, the IMF extends in a power law for around two orders of magnitude in mass (Salpeter 1955). It is tempting to speculate on the origin of the two main features of the IMF (see Larson 1995, 1996, 1998a). The slope of the upper IMF power law may be set by some scale free process. In this regard, both coagulation and competitive accretion have been cited as possible mechanisms (e.g. Murray & Lin 1996; Bonnell et al. 2001). The characteristic mass scale, on the other hand, is argued to be set by some physical property of the star forming gas and, therefore, may be expected to vary with environment and epoch (e.g. Larson 1998b).

In nearby star forming regions, the characteristic stellar mass is similar to the typical Jeans mass in dense molecular cloud cores. This Jeans mass is jointly set by the gas temperature and the pressure in the cores. Whereas the temper-

ature is fixed by the detailed physics of heating and cooling in molecular gas, the thermal pressure in the cores is apparently in a state of rough pressure balance with the mean internal pressure of bulk motions ('turbulence') within the parent molecular cloud (Larson 1996, 1998a). This conjecture has subsequently been supported by hydrodynamic simulations of turbulent clouds. These numerical experiments show that the density field generated by driven supersonic turbulence in an isothermal medium gives rise to a characteristic density at which the thermal pressure roughly balances the turbulent pressure in the cloud (e.g. Padoan, Nordlund & Jones 1997; Padoan & Nordlund 2002). Through analysis of the cloud's steady state density distribution, and by converting density to corresponding isothermal Jeans mass, these authors derive a characteristic mass and (approximately log-normal) IMF for the cloud. Similar conclusions may be derived from the recent simulations of Bate, Bonnell & Bromm (2002a,b, 2003). This work differs from the above both in that the turbulence is not driven (but allowed to decay on roughly a cloud free-fall time) and also, more crucially, in that it follows the collapse and fragmentation of gravitationally unstable gas down to the opacity limit and hence directly simulates the building up of the IMF by combined fragmentation and competitive accretion. In this case also, the mean stellar mass appears to be set by the gas temperature and the turbulent pressure of the initial conditions. For observed molecular clouds with the typical internal pressure ($nT \sim 3 \times 10^5 \text{ K cm}^{-3}$) and temperature ($\sim 10 \text{ K}$) of molecular gas cooled by CO line emission the characteristic stellar mass is around a solar mass.

In order to extend this argument so as to predict the characteristic mass scale for star formation at other epochs, and in different environments, it is evidently necessary to

consider the factors determining both the gas temperature and the mean pressure within star forming complexes. The former issue has been considered by numerous authors with the well known result that higher mass stars are to be expected at high redshift, both due to inefficient cooling of primordial gas and also to the raising of the floor set by the temperature of the cosmic microwave background (e.g. Schwarzschild & Spitzer 1953; Larson 1986, 1998b). The role of pressure variations has received less attention, partly because of the much weaker (inverse square root) dependence of the Jeans mass on pressure compared with that on temperature.

In nearby molecular clouds, two factors appear to be relevant in setting the pressure. First, it is evident that the attainment of the low temperatures needed for star formation requires that molecular coolants are self-shielded against photodissociation by the ambient UV field (e.g. van Dishoeck & Black 1988). This imposes a minimum column density for molecular clouds of around $3 \times 10^{21} \text{ cm}^{-2}$. In a self-gravitating system in which the flow velocities are comparable to their free-fall values, the pressure depends on the column density according to $P \sim G\Sigma^2$ and thus the self-shielding requirement translates into a minimum viable pressure of around $2 \times 10^4 \text{ K cm}^{-3}$. On the other hand, it is also apparent that the ambient pressure of the interstellar medium (ISM) plays a role in setting a lower limit to the mean internal pressure. Local giant molecular clouds (GMCs) are somewhat self-gravitating and the internal pressure of molecular clouds thus exceeds the ambient pressure by around an order of magnitude. The pressure within GMCs (or, equivalently, their column densities) does however appear to scale with the ambient interstellar pressure, in that the pressures within GMCs in the Galactic centre are significantly higher than those in local clouds (Sanders, Scoville & Solomon 1985). In the following, we hypothesise that the pressure in star forming environments modestly exceeds that of the ambient ISM.

Whereas we here focus on possible variations in the stellar IMF, we do not address the history of the cosmic star formation rate (SFR). This problem has been investigated by many authors, both analytically and numerically (e.g. Norman & Spaans 1997; Barkana & Loeb 2000; Springel & Hernquist 2003). A physical understanding of the cosmic SFR crucially depends on the nature of the feedback exerted by star formation on its surroundings. The character of this feedback is in turn determined by the underlying IMF. The results from our study therefore provide an important ingredient to the overall effort to elucidate the star formation history of the universe.

In this paper, we estimate the characteristic stellar mass associated with bursts of star formation accompanying the formation of galaxies. To this end, we consider the typical gas pressure and temperature in protogalaxies as they collapse and virialise. In the context of a hierarchical model of cosmic structure formation, we evaluate how the characteristic stellar mass varies as a function of collapse redshift and halo mass. Specifically, we assume a Λ CDM cosmology with density parameters in matter $\Omega_m = 1 - \Omega_\Lambda = 0.3$, and in baryons $\Omega_B = 0.045$, a Hubble constant of $h = H_0/100 \text{ km s}^{-1} \text{ Mpc}^{-1} = 0.7$, and a scale-invariant power spectrum of density fluctuations with an amplitude $\sigma_8 = 0.9$ on a scale of $8 \text{ h}^{-1} \text{ Mpc}$.

2 STAR FORMATION MODEL

In what follows, we adopt the view that the internal pressure in star forming systems at different cosmological epochs is approximately determined by the ambient pressure in the ISM. In particular, we will be focusing on the bursts of star formation that accompany the first collapse of gas into dark haloes during the assembly of galaxies. We use insights from recent numerical simulations into the thermodynamic behaviour of gas in dark haloes virialising at high redshifts (Bromm, Coppi & Larson 1999, 2002; Abel, Bryan & Norman 2002).

As overdensities in the dark matter distribution turn around from the mean cosmic expansion and collapse, the baryons they contain are initially heated by adiabatic compression. For a halo virialising at redshift z , the dark matter density at the point of virialisation is:

$$\rho_{\text{vir}} \simeq 200\rho_b(1+z)^3, \quad (1)$$

where

$$\rho_b = 2 \times 10^{-29} h^2 \Omega_m \text{ g cm}^{-3}$$

is the density of the background Universe. Assuming a cosmic ratio of baryons to dark matter of 0.15, the baryonic density at this point is:

$$n_1 \simeq 0.3 \text{ cm}^{-3} \left(\frac{1+z_{\text{vir}}}{20} \right)^3. \quad (2)$$

At this stage the temperature attained through adiabatic compression, $T \sim 500 \text{ K}$, is considerably less than the virial temperature of the halo (see Barkana & Loeb 2001)

$$T_{\text{vir}} \simeq 2000 \text{ K } M_6^{2/3} \left(\frac{1+z_{\text{vir}}}{20} \right), \quad (3)$$

where $M_x = M/10^x M_\odot$. The baryons, not being pressure supported in such a well, thus contract and continue to heat up. The further evolution depends on the mass of the halo. In the case of low mass haloes, the gas can attain a temperature of $\sim T_{\text{vir}}$ by adiabatic compression alone. The corresponding density can readily be estimated by extrapolating the adiabat from the thermodynamic state at $z = 100$ ($n \simeq 0.1 \text{ cm}^{-3}$, $T \simeq 200 \text{ K}$) to T_{vir} :

$$n_2 \simeq 3 \text{ cm}^{-3} M_6 \left(\frac{1+z_{\text{vir}}}{20} \right)^{3/2} \quad (4)$$

A different evolutionary path is followed in the case of high mass haloes, however, since centrifugal effects become important in halting radial collapse. We may estimate the halo mass at which this occurs by equating the maximum density attained in quasi-spherical collapse ($\sim n_1/\lambda^3$, where λ is the usual spin parameter) to n_2 derived above, and find a critical halo mass of

$$M_c \simeq 10^8 M_\odot \left(\frac{1+z_{\text{vir}}}{20} \right)^{3/2} \lambda_{0.1}^{-3}. \quad (5)$$

Here, the spin parameter is normalised to a fiducial value of 0.1, close to what is found in cosmological simulations (e.g. Padmanabhan 1993). In such massive haloes, once radial contraction is slowed by centrifugal support, shocks develop as infalling gas joins the incipient disc. The introduction of entropy in shocks causes the evolution in the $[n, T]$ plane to steepen with respect to the slope of adiabatic evolution, and we estimate the approximate postshock parameters to be: $n \simeq n_1/\lambda^3$ and $T \simeq T_{\text{vir}}$.

Thus, to summarise, prior to the onset of cooling, the gas arrives at a state with temperature $T_v = T_{\text{vir}}$ and density $n_v = \min(n_2, n_1/\lambda^3)$, where the relevant density depends on whether the halo mass is less than or greater than M_c . For $M < M_c$, rotational support is negligible in the virial state, whereas in the opposite limit, rotation, thermal and gravitational effects are all comparable prior to the onset of cooling.

The subsequent evolution depends on the efficiency of cooling at conditions corresponding to n_v, T_v . In general, the gas in a virialised dark matter (DM) halo will continue to collapse and fragment if the criterion $t_{\text{cool}} < t_{\text{ff}}$ is satisfied (Rees & Ostriker 1977). Systems with halo masses in excess of $\sim 10^6 M_\odot$ fulfil the Rees-Ostriker criterion either if H₂ cooling is effective (implying the absence of a sufficiently strong photodissociating UV field) or else, in the absence of photoionisation heating, if the metallicity exceeds $\simeq 10^{-3.5} Z_\odot$ (Omukai 2000; Bromm et al. 2001). More massive systems, with $M \gtrsim 10^8 M_\odot [(1+z)/10]^{-1.5}$, are able to collapse via atomic hydrogen lines (e.g. Madau, Ferrara, & Rees 2001; Oh & Hauman 2002). In each case, we assume that the gas is compressed roughly *isobarically* as it cools. Below, we discuss how the results of numerical simulations lend support to this idealized model. During the isobaric phase the pressure is

$$P_v \simeq 10^7 k_B \times \min(M_8^{5/3} \left(\frac{1+z_{\text{vir}}}{20}\right)^{5/2}, 2M_8^{2/3} \left(\frac{1+z_{\text{vir}}}{20}\right)^4 \lambda_{0.1}^{-3}) \text{ K cm}^{-3} \quad (6)$$

A similar dependence of gas pressure on mass and redshift compared to our high-mass case has been found by Norman & Spaans (1997). These authors have studied the properties of protogalactic discs, and it is therefore not surprising that our high-mass case, where centrifugal support is important, leads to a similar overall scaling.

We assume that the immediate progenitor of a star is a centrally concentrated, self-gravitating core (Motte, André, & Neri 1998) with a mass close to the Bonnor-Ebert value (e.g. Palla 2002)

$$M_{\text{BE}} \simeq 700 M_\odot \left(\frac{T}{200 \text{ K}}\right)^{3/2} \left(\frac{n}{10^4 \text{ cm}^{-3}}\right)^{-1/2} \quad (7)$$

To evaluate the minimum possible fragment mass, we need to determine T_{min} and n_{max} . The minimum temperature is given by

$$T_{\text{min}} = \max(T_{\text{cool}}, T_{\text{CMB}}) \quad (8)$$

where

$$T_{\text{cool}} = \begin{cases} 200 \text{ K} & \text{for H}_2 \\ 10 \text{ K} & \text{for CO} \end{cases} \quad (9)$$

Note that although throughout the paper we refer to the case that temperatures of ~ 10 K are obtained as ‘CO’ cooling, dust may also provide a means of achieving similarly low temperatures even in the absence of molecular coolants (see, e.g. Whitworth, Boffin & Francis 1998). A lower floor on the gas temperature is set by the cosmic microwave background (CMB) with

$$T_{\text{CMB}} = 2.7 \text{ K}(1+z) \quad (10)$$

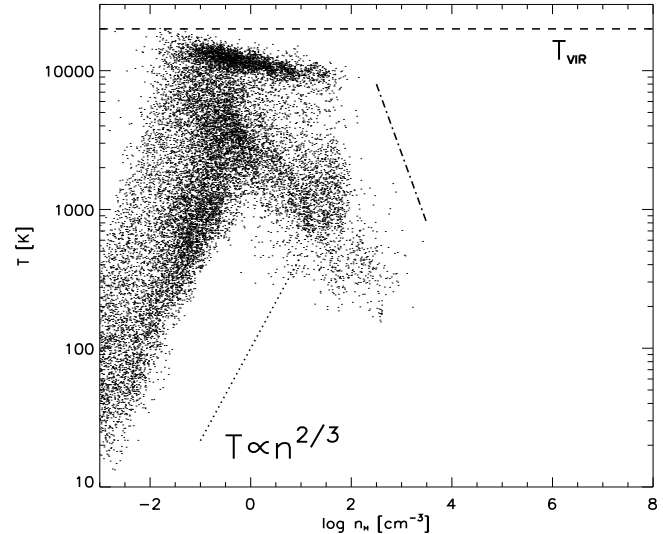


Figure 1. Thermodynamic behaviour of primordial (metal-free) gas in a dwarf-sized system. The dark halo has a total mass of $M = 10^8 M_\odot$ and collapses at $z_{\text{vir}} \simeq 10$. Shown is the gas temperature vs. hydrogen number density. At low gas densities, the temperature rises because of adiabatic compression and due to shocks until it reaches the virial value, $T_{\text{vir}} \simeq 2 \times 10^4 \text{ K}$. At higher densities, H₂ line cooling drives the temperature down again to $T \sim 200 \text{ K}$. *Dot-dashed line*: Evolution along an isobar. Notice that the cooling flow at high densities asymptotically approaches an isobaric path.

We find the maximum density by assuming that the dissipative infall proceeds along an isobar, resulting in

$$n_{\text{max}} \simeq P_v / (k_B T_{\text{min}}) \quad (11)$$

Inserting these expressions for T_{min} and n_{max} into equ. (7), we find for the low-mass case

$$M_{\text{BE}} \simeq 200 M_\odot \left(\frac{T_{\text{min}}}{200 \text{ K}}\right)^2 M_8^{-5/6} \left(\frac{1+z_{\text{vir}}}{20}\right)^{-5/4} \quad (12)$$

and for the high-mass case

$$M_{\text{BE}} \simeq 140 M_\odot \left(\frac{T_{\text{min}}}{200 \text{ K}}\right)^2 M_8^{-1/3} \left(\frac{1+z_{\text{vir}}}{20}\right)^{-2} \lambda_{0.1}^{3/2} \quad (13)$$

Depending on the details of how the gas is accreted onto the nascent protostar in the centre of the collapsing core, the resulting stellar mass is expected to be somewhat smaller than the Bonnor-Ebert mass. We take this uncertainty into account by expressing the final characteristic mass as

$$M_{\text{char}} \simeq \alpha M_{\text{BE}} \quad (14)$$

and choose the efficiency to be $\alpha \simeq 0.5$. This value is close to that inferred for the formation of stars in the present-day Universe (McKee & Tan 2002). This choice of efficiency reproduces the high redshift (Pop III) point, estimating the typical mass of such a star to be a few hundred M_\odot , collapsing in a halo of total mass $\sim 10^6 M_\odot$ at $z \sim 20$ (Bromm et al. 1999, 2002; Nakamura & Umemura 2001; Abel et al. 2002).

Clearly, this model is highly idealised, and serves only to provide an order of magnitude estimate for typical densities and pressures to be expected in regions of gas collapsing in proto-galactic potentials. Some support for this schematic evolution in the $[n, T]$ phase diagram is provided by the

results of numerical simulations of the formation of dwarf galaxies at high redshifts. For example, Figure 1 depicts the phase diagram for gas collapsing in a dark halo of mass $10^8 M_\odot$ that virialises at $z \sim 10$. This calculation is similar to that described in Bromm & Clarke (2002), except that in the case presented here it is assumed that molecular hydrogen is not photodissociated, and that the gas is metal-free. The only effective coolant at temperatures below 10^4 K is then molecular hydrogen (e.g. Tegmark et al. 1997).

Figure 1 shows that the evolution can be loosely described as adiabatic compression followed by roughly isobaric compression from the virialised state. In fact, since the halo mass in this case is quite close to the transition mass in equation (5), one can already see that shock heating is of some importance prior to virialisation, causing the path in the $[n, T]$ plane to be somewhat steeper than an adiabat at this stage. Following virialisation, the gas approximately evolves along an isobar. Note that this gas is not initially self-gravitating but is pressure confined by the weight of the overlying baryons. This roughly isobaric behaviour can be understood as follows: although the cooling timescale, t_{cool} , is less than the free-fall timescale, t_{ff} , it is longer than the sound-crossing time. Thus there is sufficient time, as the gas cools, for the passage of sound waves to maintain roughly isobaric conditions. Such an isobaric evolution has been predicted for pregalactic shocks that are able to cool via H_2 (e.g. Shapiro & Kang 1987). Applying our model to the system described in Figure 1, the predicted density at the minimum temperature (200 K) is around 100 cm^{-3} , in fair agreement with the simulation.

Our simple model is in effect a one-zone model, whereas the gas in a given dark matter halo will have a pressure and density that is dependent on radius. To constrain the possible influence of a radial pressure profile on the predicted characteristic stellar mass, we have evaluated the gas pressure in the simulation of Fig. 1. We find that the pressure is roughly independent of radius within the central ~ 150 pc, and drops by one order of magnitude out to a radius of ~ 400 pc. The characteristic stellar mass in the center of the incipient dwarf galaxy, therefore, varies only within a factor of a few due to the radial drop in pressure. We emphasize that our model is not able to reliably assess possible spatial variations in the IMF, and a more sophisticated approach would be needed to do so.

The above argument (that the pressure in the protogalaxy is set by the weight of overlying baryons) can however be generalised beyond the situation depicted in Figure 1. In this simulation, the gas is never in a state of hydrostatic equilibrium: gas in the inner regions that can cool responds to the weight of overlying gas by increasing its density to match the pressure imposed from above. We note that any bulk ('turbulent') motions induced in the collapse that are gravitational in origin (e.g. Abel et al. 2002) will introduce a ram pressure whose magnitude is at most comparable with this gravitational pressure. Likewise, in any galaxy whose gas subsequently attains a state of hydrostatic equilibrium, the central pressure (or, in a disc system, pressure in the mid-plane) adjusts to a similar value, regardless of the microphysics of the processes providing this pressure. For example, in the disc of the Milky Way (where the ambient pressure has significant contributions from cosmic rays, magnetic fields and thermal pressure) the *value* of this pressure

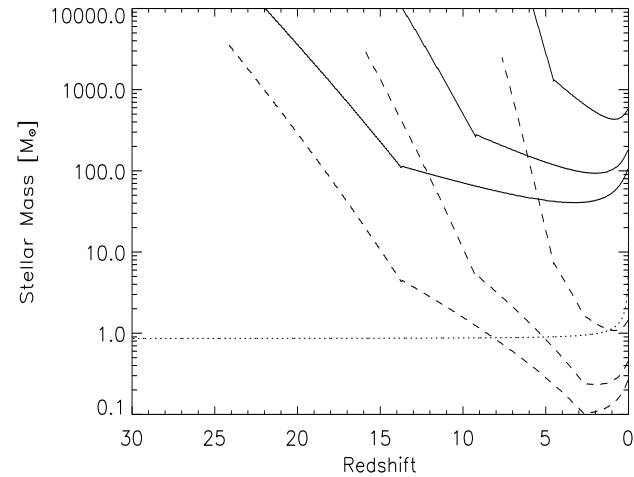


Figure 2. Evolution of characteristic stellar mass in collapsing DM haloes. Shown is the characteristic mass (in units of M_\odot) for various overdensities vs. redshift. *Solid lines*: Cooling is due to H_2 with a minimum temperature of 200 K. *Long-dashed lines*: Cooling is due to CO with a minimum temperature of 10 K. For each assumption on the cooling, the curves correspond (from top to bottom) to 1σ , 2σ , and 3σ perturbations, as shown in Fig. 4. *Dotted line*: Maximum mass of a star formed at a redshift z that would have survived to the present time.

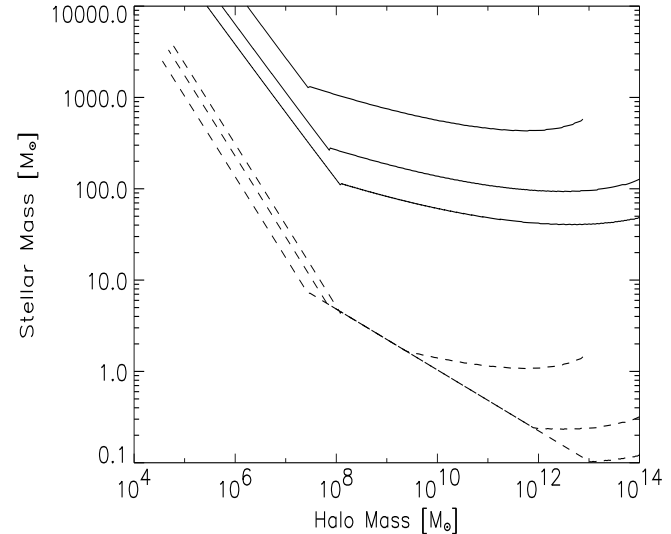


Figure 3. Evolution of characteristic stellar mass in collapsing DM haloes. Shown is the characteristic mass (in units of M_\odot) for various overdensities vs. total (DM + gas) halo mass (also in units of M_\odot). For the different lines, we adopt the same convention as in Fig. 2.

$(2.8 \times 10^4 \text{ K cm}^{-3})$ is simply given by the requirement that it supports the weight of the ISM. We have argued in Section 1 that in any galaxy this ambient pressure sets a lower limit to the internal pressure of self-gravitating, potentially star forming, clouds and that this pressure affects the Jeans mass of stars forming from cooled gas in these clouds.

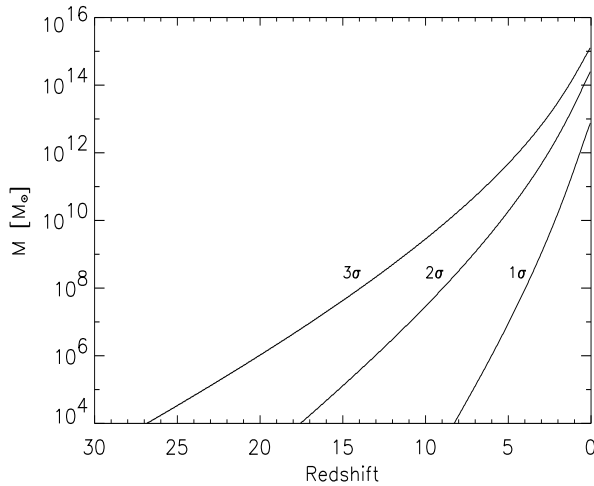


Figure 4. Gravitational evolution of cold dark matter haloes. Shown is the total halo mass for various overdensities vs. redshift. The curves are calculated for a Λ CDM spectrum with $\sigma_8 = 0.9$ and $h = 0.7$.

3 RESULTS

In Figure 2 we plot the predicted dependence of characteristic stellar mass on the redshift of virialisation of the parent halo. Each line represents the characteristic stellar mass for haloes virialising at a given redshift that lie on a locus of constant overdensity in the random field of primordial density perturbations. In order to deduce the mass of the parent halo in which such stars are formed, Figure 2 should be examined in conjunction with Figure 4, which depicts the relationship between halo mass and virialisation redshift along lines of constant overdensity for a Λ CDM model.

The solid lines represent the case that gas cannot cool below 200 K, thus approximating the case of cooling by molecular hydrogen. The solid lines, therefore, are applicable to haloes which are both low metallicity and are not subject to a strong background of photons in the Lyman-Werner range which can dissociate molecular hydrogen. In each case, the dependence of characteristic stellar mass on redshift flattens for haloes more massive than about $10^8 M_\odot$ (see equ. (5)). The reason for this change is that for lower mass haloes gas is compressed nearly adiabatically to the virial state; as the redshift of virialisation declines, the halo mass increases steeply (Figure 4) and the strongly increasing pressure manifests itself as a marked decline in the characteristic stellar mass with decreasing redshift. For haloes more massive than about $10^8 M_\odot$, however, the role of angular momentum in halting the collapse weakens the mass dependence of the virial pressure (equ. (6)), and the characteristic stellar mass declines more gently with decreasing redshift. The ordering by mass of the curves for various overdensities (i.e. higher characteristic masses for lower σ fluctuations) is simply a result of the lower pressure attained, at a given redshift, in the smaller mass haloes found in lower σ fluctuations.

The dashed lines correspond to the case that the gas can cool to the maximum of the ambient CMB temperature and a temperature of 10K, this latter representing a fiducial value for cooling by CO and dust in Population I

regions not subject to strong radiative heating by massive stars. These lines are all terminated at the high redshift end at the point where the predicted characteristic stellar mass is comparable to the total baryonic mass of the halo concerned, and are evidently only applicable well to the right of these points. Unlike the case of molecular hydrogen cooling described above, the temperature along these curves is set by the CMB for all $z > 2.7$. The decline in temperature towards the present epoch accounts for the steeper decline in characteristic stellar mass with decreasing redshift than in the H_2 cooling case, although again there is a mild flattening of the curves for haloes more massive than $10^8 M_\odot$. At low redshift ($z < 2.7$), the temperature attains a plateau value of 10K. At these low redshifts, the virial pressure *decreases* with decreasing redshift, because the explicit redshift dependence in equation (6) is more significant than the increase of halo mass with decreasing redshift. Consequently, the characteristic stellar mass rises modestly for $z < 2.7$.

Figure 3 depicts the same information as a function of halo mass, again for curves of constant overdensity and for the two different assumed coolants. This plot shows explicitly the weaker dependence of characteristic stellar mass on halo mass for haloes more massive than $\sim 10^8 M_\odot$. In the case of CO cooling in haloes more massive than $10^8 M_\odot$, but at $z > 2.7$, the characteristic stellar mass is independent of z , because the z dependence of the pressure (equ. (6)) and that of the temperature of the CMB cancel each other out in their contribution to the resulting stellar mass. Consequently, curves of different overdensity follow the same dependence of characteristic stellar mass on halo mass in this regime. For each line of constant overdensity, the characteristic stellar mass departs from this relation at a redshift of ~ 2.7 , where the plateau in the temperature attained causes a modest upturn in the characteristic stellar mass.

4 IMPLICATIONS

4.1 Summary of predicted behaviour

We have proposed a model that relates the masses of dark haloes and their virialisation redshift to the characteristic mass scale of stars, formed during the assembly of protogalaxies. We stress that the characteristic mass that we derive here is neither an upper- nor lower-mass cutoff, but is instead close to the mean mass. For an IMF of form similar to that seen in well observed local regions, this mass scale marks the transition between a power law index less than 2 to a near Salpeter ($\alpha = 2.35$) value.

This characteristic mass scale is identified with the Jeans mass, fixed jointly by the gas temperature (set by local cooling physics together with any floor set by the temperature of the cosmic microwave background) and pressure (set by the weight of overlying baryons as the gas collapses in the parent dark halo). This simple prescription implies a near solar characteristic mass scale for star formation at recent epochs (in line with observations), as well as reproducing the much higher mass scale ($\lesssim 10^3 M_\odot$) found in simulations of Population III haloes where the cooling is provided mainly by molecular hydrogen.

At redshifts greater than around 3, the characteristic mass scale increases with z , due partly to the increase in

temperature of the cosmic microwave background with z and partly because, along a line of constant overdensity $n\sigma$ (see Figure 4), the halo mass decreases with increasing z and hence the pressure in the halo declines. Although the Jeans mass varies only as $P^{-1/2}$, the steep decline in halo mass with increasing redshift of virialisation ensures a significant role for pressure variations in determining the characteristic stellar mass. The importance of pressure variations is evident in Figure 2: each of the dashed curves (and each of the solid curves) has an identical assumed dependence of temperature on redshift, so that the variations between these curves, at a given z , are entirely attributable to the different masses (and hence different pressures) of the dark haloes involved.

4.2 Observational consequences

In order to establish potentially observable diagnostics of such a cosmic star formation model, it is necessary not only to specify how the characteristic stellar mass varies with cosmic epoch and conditions, but also to address the variation of the functional form of the IMF. If we assume that the form of this IMF is invariant in different environments, but that the value of M_{char} may change, then evidently it is possible to probe the value of M_{char} only through observations that are sensitive to masses both below and above M_{char} (e.g. Wyse et al. 2002). In the following, we assess whether the model can be tested through a variety of observational diagnostics.

4.2.1 Formation of very massive black holes

An intriguing application of the curves shown in Figure 2 is to the formation of very massive black holes (VMBHs) in Population III haloes (Madau & Rees 2001). Recent theoretical studies of the thermodynamics in DM haloes prior to reionisation have argued for a critical metallicity threshold of around $10^{-3.5} Z_{\odot}$, such that cooling to the temperature of the CMB becomes possible only in systems that exceed this threshold (Omukai 2000; Bromm et al. 2001). In this picture, the attainment of the critical metallicity would cause the characteristic stellar mass to undergo a downward transition from a given $n\sigma$ H₂-cooling curve in Figure 2 to the corresponding $n\sigma$ CO-cooling curve at the same redshift (see also Mackey, Bromm & Hernquist 2003). Evidently, the magnitude of the jump in characteristic mass depends on the redshift at which this transition occurs. As stressed by Schneider et al. (2002), the key issue here is the fraction of the stellar population that is in the range $140-260 M_{\odot}$, since pair-instability supernovae from such stars provide a very efficient way of returning metals to the ISM. The simulations of star formation out of extremely low- Z gas to date have focused on low-mass haloes virialising at high redshift, where characteristic stellar masses are very large. The solid lines in Figure 2 illustrate that at lower redshifts, the characteristic stellar mass for extremely low- Z gas should fall, due simply to the larger pressures in the more massive haloes virialising at this epoch. For example, at redshifts in the range $10-15$, the characteristic stellar mass for primordial gas in $2-3\sigma$ peaks falls to a few hundred solar masses, suggesting that the fraction of stars undergoing pair-production supernovae

should rise at this point. We therefore conclude that it is very unlikely that an IMF biased towards very high masses could persist at redshifts less than $10-15$. According to Schneider et al. (2002), this would be sufficient to account for the density of supermassive black holes in nearby galaxies (assuming that the very massive stars formed in this high mass mode produced black holes that eventually merged into supermassive black holes in galactic nuclei), but would not produce enough remnant black holes to account for the bulk of baryonic dark matter.

4.2.2 Element ratios

In metal-poor stars formed at early epochs (which have therefore not been subject to enrichment by Type I supernovae) the ratio of α elements to iron is a sensitive probe of the IMF in the mass range of stars contributing Type II supernova progenitors (Tsujimoto et al. 1997). The value of this ‘Type II plateau’ for the $[\alpha/\text{Fe}]$ -ratio in fact constrains the IMF to have a slope very close to the Salpeter value for stars more massive than around $8M_{\odot}$. Inspection of Figure 2 shows that in our model, the characteristic stellar mass is predicted to be less than $8M_{\odot}$ for $z < 15$ provided the gas can cool down to the temperature of the CMB. The variation we predict in the characteristic stellar mass at lower redshifts would not leave any imprint on the $[\alpha/\text{Fe}]$ element ratio from Type II supernovae, provided the high mass tail of the IMF remains of Salpeter form.

4.2.3 Stellar populations in Lyman Break Galaxies

Population synthesis studies in Lyman Break Galaxies (LBGs) constrain the IMF to be of a Salpeter form down to stars of early B spectral type (Pettini et al. 2002). Figure 2 demonstrates that the characteristic stellar mass we predict at the redshift of LBGs ($z \sim 3$) corresponds to stars of much later spectral type. Again, therefore, the variations we predict for the characteristic stellar mass would have no effect on observable stellar populations in LBGs.

4.2.4 Frequency of very metal poor Galactic halo stars

The lowest metallicity stars are expected to have ages comparable with the age of the Universe and thus are all low mass ($\lesssim 0.8M_{\odot}$). The numbers of such stars, when combined with a chemical evolution model and a model for the assembly of the Milky Way, can be used to constrain the mass fraction of stars produced in this mass range at high redshift. Such an analysis by Hernandez and Ferrara (2001) concluded that the relative paucity of metal poor stars in the Milky Way argued for a small mass-fraction in low mass objects. They interpreted this in terms of a rather high $M_{\text{char}} (\sim 10M_{\odot})$ for stars originating in low mass haloes ($10^8-10^9 M_{\odot}$) at a redshift of $z = 5-10$. Such an inference is in good agreement with our model (see Figures 2 and 3).

Our model indicates that the conditions in the Universe at $z \gtrsim 5$ have already enabled the formation of low-mass stars, with typical masses of $\sim 1M_{\odot}$, provided that the gas has been sufficiently enriched with heavy elements. Two relevant observations could thus be accommodated. First, the inferred ages of the oldest globular clusters in the Galaxy

with metallicities of $\sim 10^{-2} Z_{\odot}$ imply a formation time close to the epoch of reionisation (e.g. Ashman & Zepf 2001; Cen 2001; Bromm & Clarke 2002). The second observational constraint is provided by the recent discovery of an extremely metal-poor star in the Galactic halo (Christlieb et al. 2002). The star HE0107-5240, with an iron abundance of $[\text{Fe}/\text{H}] = -5.3$, must have formed very early in the chemical enrichment history of the Universe, probably out of gas that had experienced only one previous episode of star formation. How could this low mass star have formed? Although this star is very iron-poor, it is dramatically overabundant in carbon and, to a somewhat lesser extent, in oxygen and nitrogen (e.g. Schneider et al. 2003). Taking into account the different elemental yields, it seems possible that the parent cloud out of which HE0107-5240 formed had already a metallicity in excess of the critical value required for low-mass star formation (see Mackey et al. 2003 for an alternative formation mechanism).

4.2.5 Characteristic mass scale for stars in Globular Clusters

The inferred age of the oldest globular clusters in the Galaxy, when combined with current cosmological models, implies that these systems were formed at redshifts $z \gtrsim 3$ (Gnedin, Lahav & Rees 2001), and several recent models tie their formation to an era close to the epoch of reionisation (Cen 2001; Bromm & Clarke 2002). Globular clusters represent the only systems from this era whose IMF is well constrained observationally. The observed mass function slope in the range $0.1 - 0.8 M_{\odot}$ is considerably flatter than the Salpeter slope, and thus (retaining the assumption that the IMF is always of Salpeter form above the characteristic stellar mass), this rules out a characteristic mass that is much less than $0.8 M_{\odot}$. On the other hand, the survival of globular clusters as bound entities rules out a very top heavy mass function ($M_{\text{char}} \gg 1 M_{\odot}$) due to the excessive mass loss predicted from stellar winds in this case (e.g. Kudritzki 2002). Figure 2 demonstrates that our model predicts a characteristic stellar mass around $z \sim 6$ which is roughly solar for haloes collapsing from 2σ peaks. Apparently, therefore, our model predicts suitably low characteristic masses at the formation epoch of globular clusters.

5 SUMMARY AND CONCLUSIONS

This paper has set out a new framework for predicting how the characteristic stellar mass should depend on halo mass, virialisation redshift and chemistry. At face value, it appears broadly consistent with available observational constraints and the results of numerical simulations at high redshift: in particular it predicts a characteristic stellar mass that is close to solar values at low redshifts, whilst reproducing the very large stellar masses predicted by simulations of Population III star formation. Our model differs from previous discussions of the rise in characteristic stellar mass at high redshifts in that it takes explicit account of the differing pressures expected in haloes of different masses and virialisation redshift. One consequence of this pressure dependence is the prediction that an IMF biased towards very massive values should not be able to persist at $z \lesssim 10 - 15$. This is

because the higher pressures expected in haloes virialising at lower redshift should bring the characteristic stellar mass down to values where copious metal production is expected via pair-instability supernovae, and thereafter the gas should be able to cool down to the temperature of the CMB.

In order to make further progress on testing this scenario against observations, it is obviously necessary to specify not only the variation of the characteristic stellar mass, but any variation of the functional form of the IMF. The power law form of the local IMF at high masses tempts us to speculate that the upper IMF is controlled by scale free processes, and that a roughly Salpeter tail is always to be expected at masses above the characteristic stellar mass. If this is the case, then our model is not tested by any observational diagnostics that relate exclusively to stellar progenitors above the characteristic stellar mass (for example the element ratios produced by Type II supernovae would be insensitive to the value of M_{char} if this were less than $\sim 8 M_{\odot}$). Instead, the model is best tested by any diagnostics that simultaneously probe the mass function above and below our predicted values of M_{char} . We conclude that the detailed observational consequences of this framework will only emerge once it is fully incorporated into a hierarchical merging scenario.

ACKNOWLEDGMENTS

We are grateful to Martin Haehnelt and Max Pettini for helpful discussions, as well as to Andrea Ferrara for detailed comments which improved the presentation of this paper. This work has been supported by the “European Community’s Research Training Network under contract HPRN-CT-2000-0155, Young Stellar Clusters.” VB acknowledges support by NSF grant AST-0071019. CJC gratefully acknowledges support from the Leverhulme Trust in the form of a Philip Leverhulme Prize.

REFERENCES

- Abel T., Bryan G.L., Norman M.L., 2002, *Science*, 295, 93
- Ashman K. M., Zepf S. E., 2001, *AJ*, 122, 1888
- Barkana R., Loeb A., 2000, *ApJ*, 539, 20
- Barkana R., Loeb A., 2001, *Physics Reports*, 349, 125
- Bate M.R., Bonnell I.A., Bromm V., 2002a, *MNRAS*, 332, L65
- Bate M.R., Bonnell I.A., Bromm V., 2002b, *MNRAS*, 336, 705
- Bate M.R., Bonnell I.A., Bromm V., 2003, *MNRAS*, 339, 577
- Bonnell I.A., Clarke C.J., Bate M.R., Pringle J.E., 2001, *MNRAS*, 324, 573
- Bromm V., Coppi P.S., Larson R.B., 1999, *ApJ*, 527, L5
- Bromm V., Ferrara A., Coppi P.S., Larson R.B., 2001, *MNRAS*, 328, 969
- Bromm V., Clarke C.J., 2002, *ApJ*, 566, L1
- Bromm V., Coppi P.S., Larson R.B., 2002, *ApJ*, 564, 23
- Cen R., 2001, *ApJ*, 560, 592
- Christlieb N., Bessell M. S., Beers T. C., Gustafsson B., Korn A., Barklem P. S., Karlsson T., Mizuno-Wiedner M., Rossi S., 2002, *Nature*, 419, 904
- Gnedin O. Y., Lahav O., Rees M.J., 2001, preprint (astro-ph/0108034)
- Hernandez X., Ferrara A., 2001, *MNRAS*, 324, 484
- Kroupa P., Tout C.A., Gilmore G., 1990, *MNRAS*, 244, 76
- Kudritzki R.P., 2002, *ApJ*, 577, 389

Larson R.B., 1986, MNRAS, 218, 409
 Larson R.B., 1995, MNRAS, 272, 213
 Larson R.B., 1996, in Kunth D., Guiderdoni B., Heydari-Malayeri M., Thuan T.X., eds., *The Interplay Between Massive Star Formation, the ISM and Galaxy Evolution*. Editions Frontières, Gif sur Yvette, p. 3
 Larson R.B., 1998a, in McCaughrean M.J., Burkert A., eds., *The Orion Complex Revisited*. Astron. Soc. Pac., San Francisco, in press
 Larson R.B., 1998b, MNRAS, 301, 569
 Mackey J., Bromm V., Hernquist L., 2003, ApJ, 586, 1
 Madau P., Rees M. J., 2001, ApJ, 551, L27
 Madau P., Ferrara A., Rees M. J., 2001, ApJ, 555, 92
 McKee C.F., Tan J.C. 2002, Nature, 416, 59
 Motte F., André P., Neri R., 1998, A&A, 336, 150
 Murray S.D., Lin D.N.C., 1996, ApJ, 467, 728
 Nakamura F., Umemura M. 2001, ApJ, 548, 19
 Norman C. A., Spaans M., 1997, ApJ, 480, 145
 Oh S. P., Haiman Z., 2002, ApJ, 569, 558
 Omukai K., 2000, ApJ, 534, 809
 Padmanabhan T., 1993, *Structure Formation in the Universe*. Cambridge Univ. Press, Cambridge, p. 305
 Padoan P., Nordlund Å., Jones B.J.T., 1997, MNRAS, 288, 145
 Padoan P., Nordlund Å., 2002, ApJ, 576, 870
 Palla F., 2002, in Maeder A., Meynet G., eds., *Physics of Star Formation in Galaxies*. Springer, Berlin, p. 16
 Pettini M., Rix S.A., Steidel C.C., Shapley A.E., Adelberger K.L., 2002, in van der Hucht K.A., Herrero A., Esteban C., eds., Proc. IAU Symp. 212, *A Massive Star Odyssey, from Main Sequence to Supernova*, in press
 Rees M. J., Ostriker J. P., 1977, MNRAS, 179, 541
 Salpeter E.E., 1955, ApJ, 121, 161
 Sanders D.B., Scoville N.Z., Solomon P.M., 1985, ApJ, 289, 373
 Scalo J., 1986, Fundam. Cosmic Phys., 11, 1
 Scalo J., 1998, in Gilmore G., Howell D., eds., *ASP Conf. Ser. Vol. 142, The Stellar Initial Mass Function*. Astron. Soc. Pac., San Francisco, p. 201
 Schneider R., Ferrara A., Natarajan P., Omukai K., 2002, ApJ, 571, 30
 Schneider R., Ferrara A., Salvaterra R., Omukai K., Bromm V., 2003, Nature, 422, 869
 Schwarzschild M., Spitzer L., 1953, Observatory, 73, 77
 Shapiro P. R., Kang H., 1987, ApJ, 318, 32
 Springel V., Hernquist L., 2003, MNRAS, 339, 312
 Tegmark M., Silk J., Rees M.J., Blanchard A., Abel T., Palla F., 1997, ApJ, 474, 1
 Tsujimoto T., Yoshii Y., Nomoto K., Matteucci F., Thielemann F.-K., Hashimoto M., 1997, ApJ, 483, 228
 van Dishoeck E.F., Black J.H., 1988, ApJ, 334, 771
 Whitworth A.P., Boffin H.M.J., Francis N., 1998, MNRAS 299, 554
 Wyse R.F.G., Gilmore G., Houdashelt M.L., Feltzing S., Hebb L., Gallagher J.S., Smecker-Hane T.A., 2002, New Astron., 7, 395